ISSN 1068-3356, Bulletin of the Lebedev Physics Institute, 2021, Vol. 48, No. 5, pp. 127–130. © Allerton Press, Inc., 2021.
Russian Text © The Author(s), 2021, published in Kratkie Soobshcheniya po Fizike, 2021, Vol. 48, No. 5, pp. 3–10.

Dependence of the Endpoint Energy of X-Ray Radiation on the Preliminary Temperature Change during the Pyroelectric Source Operation in the Pulsed Mode

A. N. Oleinik[a,b,*], E. V. Bolotov[a], M. E. Gilts[a], O. O. Ivashchuk[a,c], A. A. Klenin[a], A. S. Kubankin[a,c], and A. V. Shchagin[a,d]

[a] *International Science and Education Laboratory of Radiation Physics, Belgorod State University, Belgorod, 308570 Russia*

[b] *Royal Holloway College, London University, Egham, Surey, TW20 0EX, Great Britain*

[c] *Lebedev Physical Institute, Russian Academy of Sciences, Moscow, 119991 Russia*

[d] *National Scientific Center Kharkov Institute of Physics and Technology, Kharkov, 61108 Ukraine*

*****e-mail: andreyoleynik92@mail.ru*

Received September 5, 2020; revised September 15, 2020; accepted September 16, 2020

Abstract—This paper presents the results of the study of the dependence of the endpoint energy of X-ray radiation on the preliminary change in the temperature of the lithium tantalate ($LiTaO_3$) single crystal, which is a source of a strong electric field of the pyroelectric effect under vacuum conditions. Measurements were performed in a pulsed mode of X-ray generation, consisting in a preliminary change in the pyroelectric sample temperature in high vacuum and the use of an additional electron source for complete pyroelectric discharge. The obtained dependence suggests that the maximum capacity of X-ray generation by a pyroelectric source manifests itself when using the pulsed mode.

Keywords: pyroelectric effect, X-ray radiation, lithium tantalate

DOI: 10.3103/S1068335621050079

Modern science and engineering need for compact charged-particle accelerators and X-ray sources [1–3]. One of the original methods for solving this problem is the use of the pyroelectric effect in lithium niobate or tantalate single crystals [4–6] or in zirconate-lead titanate ceramics [7]. The pyroelectric effect consists in charge induction on certain sample surfaces when its temperature is varied [8]. The implementation of this effect under conditions of ambient vacuum (0.1 Torr and below) leads to a strong electric field generation near the pyroelectric followed by electron, ion, and X-ray generation [9].

One of the poorly understood fundamental aspects of the pyroelectric effect manifestation under vacuum conditions is the determination of the correlation between the maximum possible generated electric potential and the variation range of the pyroelectric temperature. As a rule, the maximum generated electric potential on the surface of the pyroelectric sample (crystal) can be estimated by the endpoint energy of the X-ray spectrum [10]. By the pyroelectric effect definition, the induced charge is directly proportional to the temperature change, which suggests the same behavior of the dependence for the generated electric potential. However, it is known that there are several mechanisms of charge leakage from the surface of the pyroelectric sample (crystal) [11] (e.g., through lateral surfaces or ambient medium), whose contribution can become more significant with electric field, thus limiting the achievable electric field. To correctly determine the dependence of the maximum electric potential on the temperature variation range, a high vacuum of 10^{-5}–10^{-6} Torr should be achieved to limit charge leakage through an ambient medium, thus creating conditions that the major portion of the charge would remained on the surface of the pyroelectric sample (crystal). However, under such pressure of residual gas, X-ray generation becomes much weaker [12], which eventually does not allow correct estimation of the maximum possible electric potential when implementing the pyroelectric effect under high vacuum conditions.

The solution of this problem can be facilitated by the recently proposed method for controlling the pyroelectric source of X-rays, consisting of source operation modulation by electron pulses from an additional source [12]. After a preliminary temperature change, electrons from the additional source are injected into the gap between the pyroelectric and target and are accelerated to this or that side, causing

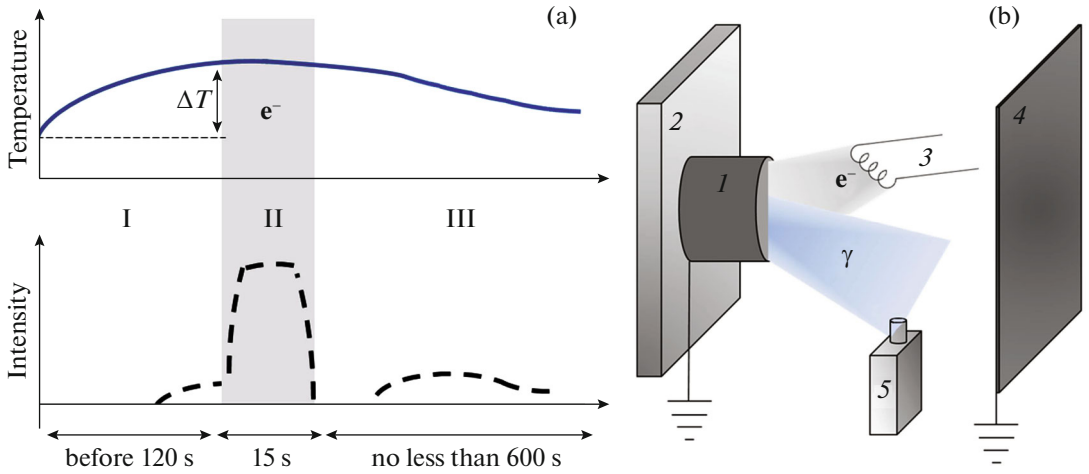

Fig. 1. (a) Variations of the pyroelectric temperature and generated X-ray intensity during the experiment. The following experimental stages are distinguished: (I) preliminary pyroelectric heating, (II) pyroelectric illumination by an additional electron emitter, and (III) natural pyroelectric cooling. (b) Schematic of X-ray generation from the surface of the pyroelectric sample (crystal) upon exposure to the additional electron emitter. (*1*) pyroelectric crystal of lithium tantalate, (*2*) Peltier element, (*3*) electron emitter (incandescent filament), (*4*) target, and (*5*) X-ray detector.

the X-ray generation effect enhancement. Such an operation makes it possible (i) to increase the peak intensity of generated radiation at least by two orders of magnitude in comparison with standard pyroelectric sources and (ii) to obtain the pulsed X-ray generation mode for a given source type. The parameters of the preliminary temperature change and additional electron injection can be varied, which allows more controllable X-ray generation during the pyroelectric effect.

In this paper, we present the results of determining the dependence of the electric potential generated during the pyroelectric effect on the free surface of the lithium tantalate single crystal (determined by the endpoint X-ray energy) on the preliminary temperature change of the pyroelectric. X-rays were generated in the pulsed mode after reaching a certain temperature change. The pyroelectric, cylindrical lithium tantalate single crystal ($LiTaO_3$) (20 mm in diameter, 10 mm in height, the spontaneous polarization vector is oriented along the cylinder axis), was oriented so that a positive charge would be induced on the free surface of the pyroelectric sample (crystal) upon heating.

Three experimental stages should be distinguished: preliminary heating, surface irradiation by an additional electron emitter, and natural cooling. The schematic variation of main experimental parameters (temperature of the pyroelectric sample (crystal) and generated X-ray intensity) during each stage is presented in Fig. 1a. The crystal was preliminarily heated using a Peltier element at a residual gas pressure of $\sim 2 \times 10^{-5}$ Torr. After completing preliminary heating, we turned the electron emmiter on for a short time (~15 s). An incandescent filament at a voltage of 1 V was used as an emitter. Electrons were accelerated to the positively charged surface of the pyroelectric sample (crystal), which led to bremsstrahlung and characteristic X-ray generation during electron stopping on pyroelectric atoms. This process is schematically shown in Fig. 1b. Afterwards, the electron emitter was turned off, the pyroelectric was naturally cooled, causing negative charge induction on the polar surface and X-ray generation under target bombardment by electrons accelerated from the surface of the pyroelectric sample (crystal). A stainless steel plate was used as a target.

Throughout the experimental time, the generated X-ray spectrum was measured using an XR-100SDD Amptek silicon drift detector, which was placed approximately at the same distance from the pyroelectric and target. The spectrum was measured in the range of 0.5–110 keV, the peak time was 4.8 μs, and the detector area was 25 mm^2. The detector was preliminarily calibrated using the ^{237}Np isotope, and the 16.65-keV linewidth at half maximum was 160 eV. The temperature near the pyroelectric lower surface was measured using a *K*-type thermocouple.

In various measurements, the preliminary pyroelectric temperature change ΔT was varied. The X-ray spectra obtained at various ΔT were compared and analyzed. Figure 2 shows the X-ray spectra measured during each experimental stage: preliminary heating by $\Delta T \approx 50$°C, operation of the additional electron emitter, and natural pyroelectric cooling. Upon preliminary heating, very weak X-ray generation is observed (the averaged intensity of detected photons is no more than 150 events per second); in this case, the radiation energy does not exceed 10 keV and no characteristic lines are observed. Based on this spec-

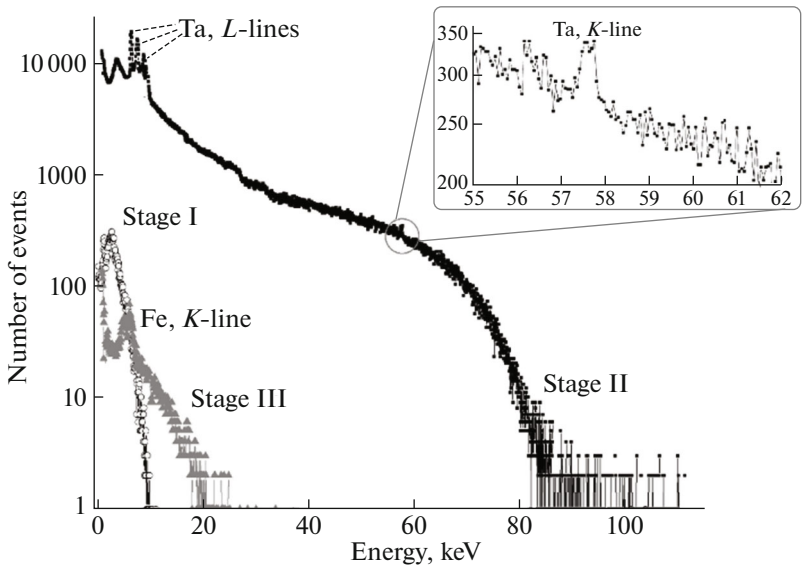

Fig. 2. X-ray spectra measured upon preliminary heating (stage I), upon exposure to an additional electron source (stage II), and subsequent natural pyroelectric cooling (stage III). The inset shows the spectral region with a characteristic tantalum *K*-line, measured during stage II.

trum, it can be concluded that the generated electric field has an insufficient strength for generating X-rays with higher energies. However, the actual cause of weak X-ray generation consists in a decrease in the number of electron sources with decreasing residual gas pressure, which promotes prolonged charge storage on the surface of the pyroelectric sample (crystal).

Actuation of an additional electron emitter in the absence of an active temperature change causes strong X-ray generation (the average intensity of recorded photons was 1.1×10^5 photons per second) with an endpoint energy of ~90 keV. Characteristic tantalum lines are observed (L_α 8.15 keV, L_β 9.34 keV, L_α 10.89 keV, as well as K_α 57.53 keV, see the inset of Fig. 2), which confirms that X-rays were emitted from the pyroelectric. Thus, X-ray emission was caused exactly by deceleration of accelerated electrons incident on the pyroelectric; in this case, during the period of the incandescent filament action, no active change in the temperature of the pyroelectric sample (crystal) and charge induction on its surface were observed, which suggests that the charge accumulated on the surface of the pyroelectric sample upon preliminary heating is the electric field source. A longer irradiation of the surface of the pyroelectric sample by an electron source is meaningless, since the entire accumulated positive charge is compensated by incident electrons.

Then, upon natural cooling, X-ray generation is observed again during negative charge induction. Characteristic lines of iron (K_α 6.40 keV) and chromium (K_α 5.41 keV) entering into the composition of stainless steel are observed; the endpoint energy reaches 20 keV.

However, the radiation intensity is by orders of magnitude weaker than that under additional pyroelectric irradiation with electrons.

A series of similar measurements with several preliminary temperature changes ΔT were performed. Figure 3 shows the target dependence of the endpoint X-ray energy, generated due to the additional electron source on the preliminary temperature change varied in the range from 10 to 60°C. The studies with temperatures varied above the indicated limit were complicated by capability of the used Peltier element, as well as by the danger of developing mechanical damages caused by excessively intense heating.

At relatively small preliminary temperature changes (~10–40°C), this dependence is linear; however, a further increase in this value leads to gradual saturation of the endpoint energy in the region of 80 keV. To all appearance, this is because of an increase in the charge fraction lost from the polar surface through an ambient medium, lateral surfaces, and pyroelectric volume as the charge induced to the polar surface of the pyroelectric sample (crystal) increases. Estimations of the endpoint electron energy with changing the lithium tantalate single crystal temperature by 50°C in the single-crystal scheme show that the maximum achievable energy is ~100 keV [5, 13], which is consistent with our results. The difference between the estimate and experimentally observed endpoint energy made it possible to estimate the lost charge fraction as 20% of the total induced charge. It should also be noted that a relatively small temperature change (~10°C) already allows observation of X-ray generation with endpoint energy of even ~40 keV.

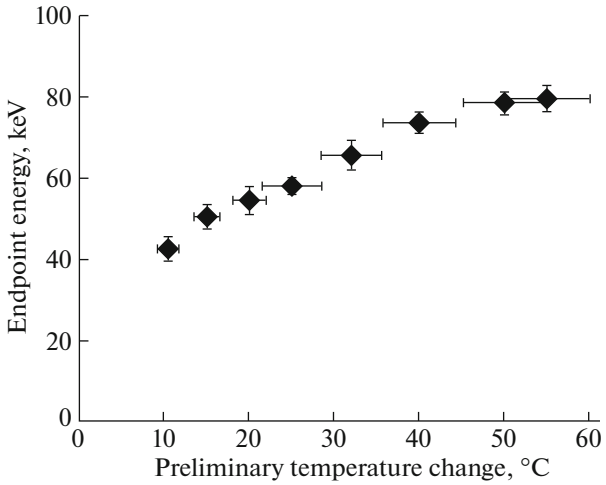

Fig. 3. Dependence of the endpoint X-ray energy generated by an additional electron source on the preliminary temperature change.

An additional temperature change by a small value causes an abrupt reduction of the X-ray generation effect, which complicates correct determination of the endpoint spectrum energy at a small preliminary temperature change.

Thus, the use of the pulsed X-ray generation mode and an additional electron emitter makes it possible to obtain the upper estimate of the endpoint X-ray energy by changing the pyroelectric temperature by a certain value. The lower X-ray energy will indicate the existence of processes resulting in increased charge leakage from the surface of the pyroelectric sample (crystal) or the absence of the balance between positive and negative charges during thermal cycling. Special attention should be paid to the fact that the measurements performed clearly show that the use of the pulsed mode of the pyroelectric source makes it possible to achieve maximum characteristics of generated radiation, which suggests that exactly these operating conditions will make use of pyroelectric X-ray sources in various applications.

FUNDING

The work of A.K. was financially supported by a Program of the Ministry of Education and Science of the Russian Federation for higher education establishments, project No. FZWG-2020-0032 (2019-1569).

REFERENCES

1. Grieken, R.V. and Markowicz A., *Handbook of X-Ray Spectrometry*, New York: Marcel Dekker, 2002.
2. Górecka-Drzazga, A., Miniature X-ray sources, *J. Microelectromech. Syst.*, 2017, vol. 26, no. 1, p. 295.
3. Russo, P., *Handbook of X-Ray Imaging*, Boca Raton: CRC Press, 2018.
4. Brownridge, J.D., Pyroelectric X-ray generator, *Nature*, 1992, vol. 358, p. 287.
5. Geuther, J.A. and Danon, Y., High-energy X-ray production with pyroelectric crystals, *J. Appl. Phys.*, 2005, vol. 97, p. 104916.
6. Kubankin, A.S., Chepurnov, A.S., Ivashchuk, O.O., et al., Optimal speed of temperature change of a crystal in a pyroelectric X-ray radiation source, *AIP Adv.*, 2018, vol. 8, p. 035207.
7. Shchagin, A.V., Miroshnik, V.S., Volkov, V.I., et al., Ferroelectric ceramics in a pyroelectric accelerator, *Appl. Phys. Lett.,* 2015, vol. 107, p. 233505.
8. Bassani, F., *Encyclopedia of Condensed Matter Physics*, Amsterdam: Elsevier, 2005.
9. Brownridge, J.D. and Shafroth, S.M., *Electron and positive ion beams and X-rays produced by heated and cooled pyroelectric crystals such as $LiNbO_3$ and $LiTaO_3$ in dilute gases:* Phenomenology and applications, in *Trends in Laser and Electro-Optic Research*, Arkin, W.T., Ed., New York: Nova Science, 2006, pp. 59–95.
10. Nagaychenko, V.I., Sanin, V.M., Yegorov, A.M., and Shchagin, A.V., Spectra of pyroelectric X-ray generator, *Vopr. Atom. Nauki Tekhn.*, 2004, vol. 412, no. 2, pp. 214–216.
11. Oleinik, A.N., Karataev, P.V., Klenin, A.A., et al., Lateral surface electrization of Z-cut lithium niobate during pyroelectric effect, *Russ. Phys. J.*, 2020, vol. 63, pp. 119–125.
12. Ivashchuk, O.O., Shchagin, A.V., Kubankin, A.S., et al., Pyroelectric accelerator and X-ray source in pulsed mode, *J. Instrum.*, 2020, vol. 15, p. C02002.
13. Geuther, J., Radiation generation with pyroelectric crystals, *Cand. Sci. Dissertation*, Troy, NY: Rensselaer Polytechnic Inst., 2007.

Translated by A. Kazantsev